CrossMark

Experimental study on kinetics of coal char–CO$_2$ reaction by means of pressurized thermogravimetric analysis

Martyna Tomaszewicz[1] · Grzegorz Tomaszewicz[1] · Marek Sciazko[1]

Abstract Comprehensive kinetic studies were performed to establish the validity of many kinetic expressions that describe the behavior of char samples during pressurized gasification toward CO$_2$. The gasification experiments were carried out isothermally in a high-pressure thermogravimetric analyzer (TG-HPs, TA Instruments, USA). Two char samples derived from Turów lignite B and Janina sub-bituminous C were used for the studies. The models that were employed are regarded as the most popular: the volumetric (VM); the modified volumetric (MVM); the grain (GM); the random pore (RPM); and the Langmuir–Hinshelwood model. The models were validated at 850, 950, and 1050 °C, and at CO$_2$ pressures of 0.4, 1, 11, and 21 bar. The effects of temperature and pressure were significant and increased the reaction rate. The calculated values of activation energy were similar for the various models employed and ranged from 169 to 212 kJ mol^{-1} for the Turów sample and 182 to 238 kJ mol^{-1} for the Janina coal char sample. The GM, RPM, and MVM fit the experimental data well, in contrast to the VM and LH models.

Keywords Reactivity · Coal char · High pressure · Kinetics · Model validation

Introduction

Due to observed global climate change, growing interest is paid to limit and control the greenhouse gases emissions, especially CO$_2$. Carbon capture and storage (CCS) and

increasing the energy generation efficiency and introduction of non-fossil fuels are approaches for reduction of CO$_2$ holding the greatest promise. Under the CCS approach, the CO$_2$ would be captured from power plants and, afterward, injected into geological formations to lock up the gas for decades [1]. Up to date, there are three technological pathways considered as the more efficient for CO$_2$ capture from coal-derived power generation: post-combustion capture with amine-based systems [2], solid sorbents based on calcium oxide [3, 4], membranes and ionic liquids; pre-combustion technologies with integrated gasification combined cycle (IGCC) and sorbents for chemical looping [5–7]; and finally, the oxy-fuel combustion technology [8, 9].

The gasification of coal is considered to be an effective and clean method to produce gas that can be used to generate power and heat and/or be used as a chemical feedstock. Two major steps can be distinguished during the gasification process: the initial rapid pyrolysis of coal to produce char, gases and tars and the subsequent gasification of the nascent char. The rate of the second step is relatively low due to the poor reactivity of char. This rate significantly affects the gasification efficiency. To improve this efficiency, a novel gasification method is being developed at the Institute for Chemical Processing of Coal (IChPW) in which additional carbon dioxide is added to the process. As indicated in the thermodynamic model, the CO$_2$ plays a dual role in the process as both a carbon and oxygen carrier [10]. The beneficial effect of the CO$_2$ addition is associated with a decrease in the demand for both carbon and oxygen while maintaining the syngas quality as in conventional air-blown systems by increasing the influence of the char–CO$_2$ reaction [10]. The process is designed to operate in a 600-kW PDU-scale pressurized circulating fluidized bed reactor rig, which is part of the

✉ Martyna Tomaszewicz
mtomaszewicz@ichpw.pl

[1] IChPW, Institute for Chemical Processing of Coal, Zabrze, Poland

Clean Coal Technologies Center of the IChPW. Hence, a thorough understanding of the char reaction kinetics is essential to optimize the process conditions, especially those of the char–CO_2 reaction, which is one of the slowest independent gasification reactions, and simultaneously plays a critical role in the proposed process conception.

Knowledge of char reactivity and understanding the char–CO_2 reaction kinetics are fundamental to both the design of gasification reactors and the optimization of process conditions. The reactivity of coal chars is influenced by many factors, such as the conditions during devolatilization, parent coal rank, pore structure and texture, mineral matter content, and its composition [11, 12]. Additionally, the pressure affects the char gasification rate, especially for chars derived from lower rank coals [13, 14].

Numerous models can sufficiently describe the CO_2 gasification rate variation, irrespective of whether the models consider the structural changes in the coal char as the reaction proceeds. The models regarded as the most popular include the volumetric; the modified volumetric; the grain (shrinking core); the random pore; and the Langmuir–Hinshelwood models.

The present work primarily aimed to characterize the kinetics of the pressurized CO_2 gasification of chars prepared from two different rank coals from Polish mines at different temperatures (850–1050 °C) and CO_2 pressures (0.4, 1, 11 and 21 bar). The second objective was to compare the results of fitting the aforementioned kinetic models to the experimental data. The paper continues the study reported before on char–CO_2 reaction kinetics, which was firstly studied by means of atmospheric thermogravimetric analyzer [15].

Experimental

Two coals, sub-bituminous C from the Janina coalmine and the lignite B from the Turów open-pit mine, were selected for this study. A thorough characterization of the studied coals in terms of proximate and ultimate analyses is given in Table 1 with the ash and maceral composition. Chars were prepared by devolatilizing the parent coals in a fixed-bed reactor heated by an electric furnace under inert gas flow (nitrogen). The samples were pyrolyzed at a heating rate of 5 K min^{-1} to a final temperature of 1000 °C; the samples were maintained at this temperature for 30 min. After cooling the char samples to room temperature under flowing nitrogen, the samples were ground and sieved, and particles less than 200 μm were used for thermogravimetric studies.

To characterize the char pore structure, a 3Flex, produced by Micromeritics, USA, was employed to determine the pore volume and surface area by means of N_2 and CO_2

adsorption isotherms at 77 and 273 K, respectively. Prior to the measurements, the samples were degassed under a vacuum at 350 °C for 4 h. The N_2 and CO_2 adsorption isotherms are presented in Fig. 1a, b, correspondingly.

Generally, the pore characteristics of solid materials is analyzed in terms of presence of three types of pores: micropores with a pore size smaller than 2 nm, mesopores with a pore diameter between 2 and 50 nm, and macropores which are pores wider than 50 nm. By analyzing the nitrogen adsorption/desorption curve (Fig. 1a) for both Janina and Turów char samples, type-II isotherms are observed. However, in case Turów coal char, no hysteresis loop was registered indicating of very complex pore characteristics. In case of Janina coal char, no micropores to be penetrated by nitrogen are present, so the isotherm increases gradually until relative pressure of 0.9 is reached. However, for Turów coal char adsorption of nitrogen in micropores is observed. The surface area was calculated by the BET method for experiments with nitrogen adsorption. The Dubinin–Astakhov theory (D–A) was employed to calculate the volume and surface area of micropores inaccessible for nitrogen adsorption at 77 K, which were filled during adsorption of CO_2 at 273 K (Fig. 1b). The big differences in results obtained with both adsorptives for Janina coal char indicate that some micropores are present, but they are so small that nitrogen molecules cannot penetrate them. The results of the pore characteristics are summarized in Table 2.

The kinetic measurements were conducted in a TG-HPs high-pressure thermogravimetric analyzer (TA Instruments, USA), which is shown in Fig. 2. The gasification experiments were performed isothermally between 850 and 1050 °C at pressures of 1, 11, and 21 bar. Moreover, experiments were also conducted at a CO_2 partial pressure of 0.4 bar using a mixture of 40% CO_2 in helium at a total pressure of 1 bar. A weighed (50 mg) char sample was placed inside the alumina crucible. The flow of the gasifying agent (CO_2 or CO_2/He mixture) was set to 1000 mL min^{-1} for all experiments.

An exemplary chart including the TG curve as well as recorded temperature and pressure signals is given in Fig. 3 below for Janina and Turów chars gasified at 950 °C and 11 bar$_a$. Please note that pressure signal is given as overpressure, so it does not include value of ambient pressure.

The carbon conversion degree was determined by means of Eq. 1:

$$X = \frac{w_0 - w}{w_0 - w_{ash}} \tag{1}$$

where w_0, w, and w_{ash} are the initial mass of char, the instantaneous mass of char and the mass of ash remaining after complete carbon conversion was reached, respectively.

Table 1 Characterization of parent coals by the means of proximate and ultimate analyses, chemical composition of ash, maceral composition and reflectance

	Parameter	Method	Procedure (Standard)	Turów LigB	Janina SubC
Proximate analysis/mass%	M_T^{ar}	Distillation for lignite, mass loss for higher rank coals	PN-EN ISO 9029:2005 PN-80/G-04511	44.2	21.3
	M^{ad}	Thermogravimetric	PN-G-04560:1998	3.9	12
	A^d			8.1	12.0
	VM^{daf}	Mass loss	ISO 562:2010	59.14	39.56
Ultimate analysis/mass%	C_T^{ad}	High-temperature tube furnace combustion with infrared absorption	ISO 29541:2010	62.3	60.4
	H_T^{ad}			5.48	3.46
	N^{ad}	High-temperature tube furnace combustion with thermal conductive detection	ISO 29541:2010	0.61	0.94
	S_T^{ad}	High-temperature tube furnace combustion with infrared absorption	ISO 19579:2006	1.02	1.22
	S_A^{ad}		PN-G-04584:2001	0.28	0.05
	S_C^{ad}	By difference		0.74	1.17
	O_{diff}^{ad}	By difference	ASTM D-3176	19.17	11.23
Chemical composition of ash/mass%	SiO_2	Inductively coupled plasma optical emission spectrometry (ICP-OES)	ASTM D-6349	32.7	46.48
	Al_2O_3			24.5	28.42
	Fe_2O_3			11.4	9.59
	CaO			4.10	3.33
	MgO			6.24	2.76
	TiO_2			1.86	1.11
	Na_2O			6.76	3.49
	K_2O			NDA	2.46
Maceral composition/%	V	Microscopic analysis	PN-ISO 7404-3:2001	73	65
	L			17	10
	I			6	18
Reflectance/%	R_o		PN-ISO 7404-5:2002	0.23	0.44

M, total moisture content; A, ash content; VM, volatile matter content; C_T, total carbon content; H_T, total hydrogen content; N, nitrogen content; S_T, total sulfur content; S_A, content of inorganic sulfur (combined with mineral matter); S_C, content of organic sulfur (combined with organic matter); O_{diff}, oxygen content calculated by difference; V, vitrinite content; L, liptinite content; I, inertinite contents; ar, as-received basis; ad, air-dried basis; d, dry basis; daf, dry and ash-free basis

Kinetic models

Many models describe changes in the gasification rate of carbonaceous materials, which are derived by modifying a global kinetic expression that is defined as follows:

$$\frac{dX}{dt} = k(T, P_{CO_2})f(X) \tag{2}$$

where dX/dt is the reaction rate, k is the reaction rate constant that considers the effect of temperature (T) and gasifying agent pressure (P_{CO_2}), and $f(X)$ denotes a term expressing the physical changes of the solid occurring as the reaction proceeds. The rate constant depends on the temperature by means of an Arrhenius-type relationship with the reaction order (m), which represents the effect of pressure of CO_2. This expression is given by Eq. 3:

$$k = AP_{CO_2}^m \exp\left(-\frac{E}{RT}\right) \tag{3}$$

where A is the pre-exponential factor, E is the activation energy, R is the universal gas constant, and T is the reaction temperature.

Several models are employed in the present study to describe the changes in the gasification rate. These models generally differ with respect to their formulation of the term $f(X)$.

The Volumetric Model (known also as the I-order kinetic model) assumes a homogeneous reaction throughout the whole particle and a linearly decreasing reaction surface area with conversion [17]. The overall reaction rate is expressed by:

$$\frac{dX}{dt} = k_{VM}(1 - X) \tag{4}$$
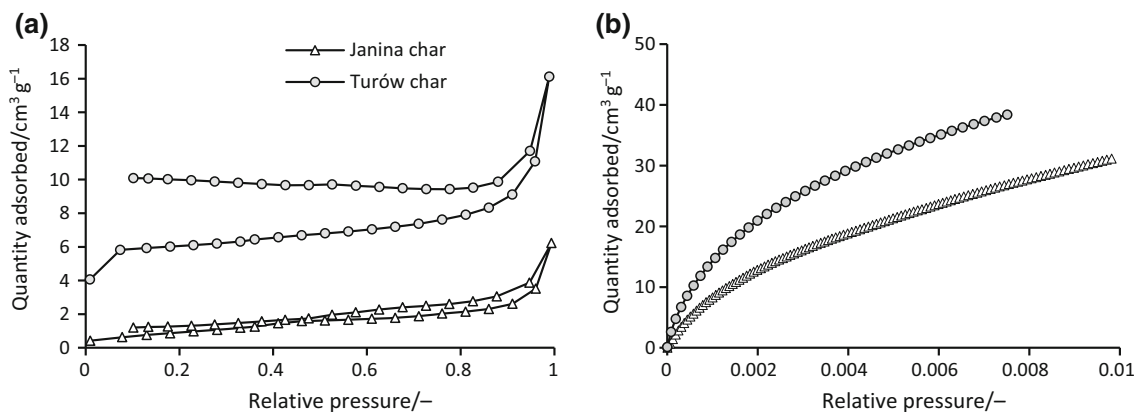
Fig. 1 Nitrogen (a) and carbon dioxide (b) adsorption isotherms for studied samples

Separating the variables yields a linearized expression that can be used to estimate the kinetic constant:

$$-\ln(1 - X) = k_{\mathrm{VM}} \cdot t \tag{5}$$

The Grain Model or shrinking-core model, introduced by Székely and Evans [18], assumes that a porous particle consists of an assembly of uniform, individual nonporous grains and that the reaction takes place on the surface of these grains. The porous network is formed by interparticle voids between these grains. The shrinking-core behavior applies to each of these grains during the reaction. Assuming kinetic control and that the grains are spherical, the overall reaction rate in these model is expressed as follows:

$$\frac{\mathrm{d}X}{\mathrm{d}t} = k_{\mathrm{GM}}(1 - X)^{\frac{2}{3}} \tag{6}$$

This model predicts a monotonically decreasing reaction rate and surface area because the surface area of each grain is receding during the reaction. The linearized expression is given by Eq. 7:

$$3\left(1 - (1 - X)^{\frac{1}{3}}\right) = k_{\mathrm{GM}} \cdot t \tag{7}$$

The Random Pore Model developed by Bhatia and Perlmutter [19] considers the overlapping of pore surfaces, which results in significant variability of the area available for reaction as the degree of conversion increases [18]. The basic equation for this model is:

$$\frac{\mathrm{d}X}{\mathrm{d}t} = k_{\mathrm{RPM}}(1 - X)\sqrt{1 - \psi \ln(1 - X)} \tag{8}$$

This model can predict a maximum in the reactivity as the reaction proceeds because it considers the competing effects of pore growth during the initial stages of gasification and the destruction of the pores due to the coalescence of neighboring pores for higher conversions of carbon. The RPM model defines a structural parameter, ψ, which is directly related to the pore structure of the initial sample by means of Eq. 9:

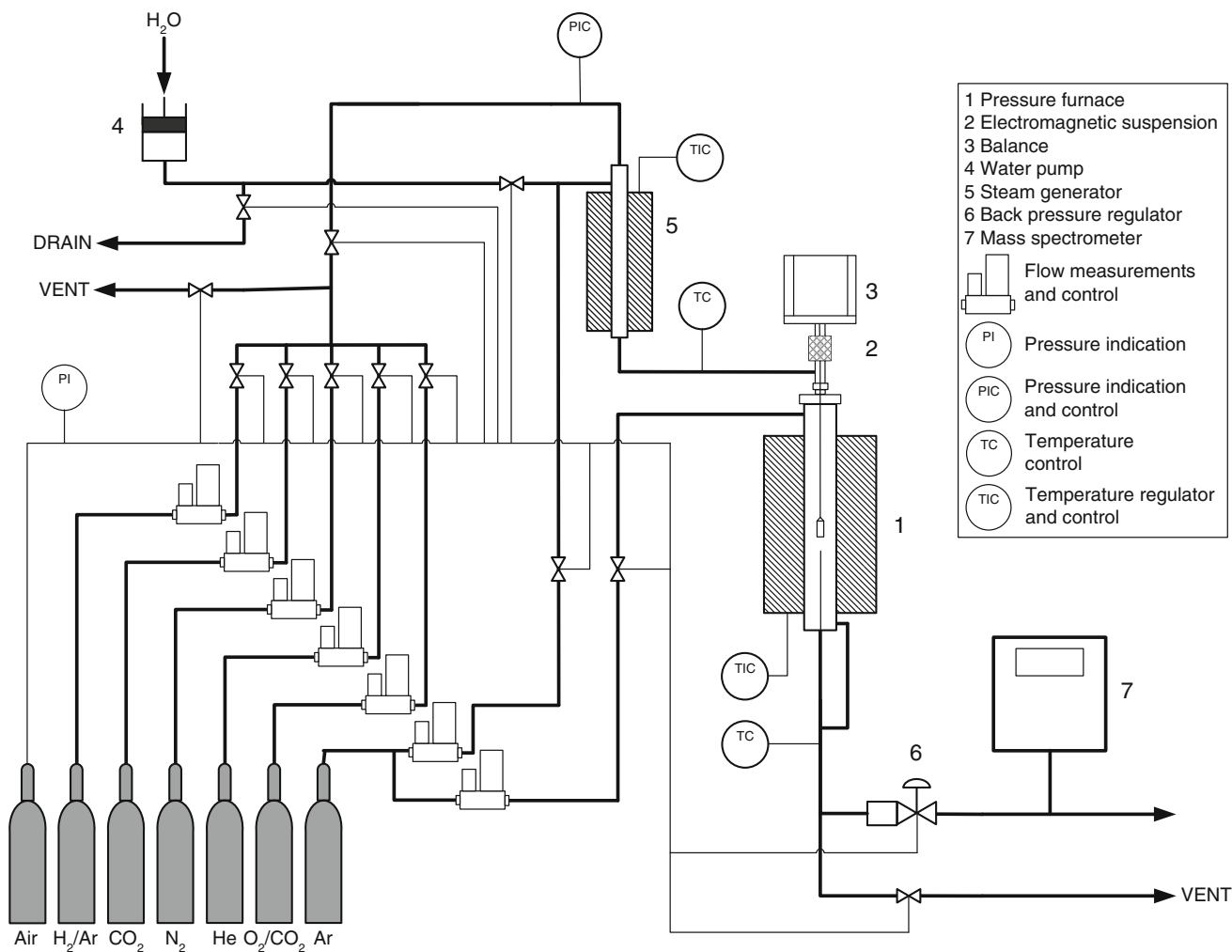$$\psi = \frac{4\pi L_0(1 - \varepsilon_0)}{S_0^2} \tag{9}$$

where S_0, L_0, and ε_0 represent the pore surface area, pore length, and solid porosity, respectively. Another method to calculate ψ is based on experimental data and uses the experimental conversion value at which the reaction rate is maximized, $X_{\max}$. By differentiating Eq. 8, ψ can be estimated in terms of $X_{\max}$ as follows:

$$\psi = \frac{2}{2\ln(1 - X_{\max}) + 1} \tag{10}$$

The following expression is used to calculate the reaction rate constant:

$$\frac{2}{\psi}\left(\sqrt{1 - \psi \ln(1 - X)} - 1\right) = k_{\mathrm{RPM}}t \tag{11}$$

The modified volumetric model (MVM) was first introduced by Kasaoka et al. [20] as an empirical modification of the VM. However, the MVM assumes that the rate constant is changing with conversion of the solid (X) as the reaction proceeds [20]. The reaction rate can be expressed

Table 2 Pore characteristics of the coal chars used for experiments

Parameter	Turów char	Janina char
Nitrogen adsorption at 77 K		
$S_{\mathrm{BET}}/\mathrm{m}^2\ \mathrm{g}^{-1}$	17.3	3.8
$V_{\mathrm{T}}/\mathrm{cm}^3\ \mathrm{g}^{-1}$	0.0154	0.0448
$V_{\mathrm{mi}}/\mathrm{cm}^3\ \mathrm{g}^{-1}$	0.0091	0.0011
$V_{\mathrm{me}}/\mathrm{cm}^3\ \mathrm{g}^{-1}$	0.0063	0.0438
Carbon dioxide adsorption at 273 K		
$S_{\mathrm{D-A}}/\mathrm{m}^2\ \mathrm{g}^{-1}$	719.31	312.9
$V_{\mathrm{D-A}}/\mathrm{cm}^3\ \mathrm{g}^{-1}$	0.2055	0.0322

Fig. 2 Scheme of the TA Instruments TG-HPs high-pressure thermogravimetric analyzer used for studies on gasification kinetics (reprinted from [16] with kind permission of Elsevier)

by means of Eq. 12 and the change in conversion degree with Eq. 13:

$$\frac{\mathrm{d}X}{\mathrm{d}t} = k_{\mathrm{MVM}}(X)(1 - X) \tag{12}$$

$$-\ln(1 - X) = at^{\mathrm{b}} \tag{13}$$

where $k_{\mathrm{MVM}}(X)$ is the model-corresponding kinetic constant, and a and b are the empirical parameters. The constant b is considered related to the physical structure of chars, while the constant a is regarded to be more closely related to the intrinsic reactivity of chars [19]. The rate constant k_{MVM} can be calculated by using Eq. 14:

$$k_{\mathrm{MVM}}(X) = a^{\frac{1}{b}}b[-\ln(1 - X)]^{\frac{b-1}{b}} \tag{14}$$

The above expression can be integrated to obtain a mean value of the rate constant, which can be useful to obtain the kinetic parameters by means of Eq. 3 and comparing other constants derived from the analysis of kinetic expressions. Equation 15 gives the formulation for the integration:

$$\overline{k}_{\mathrm{MVM}} = \int\limits_{0}^{1} k_{\mathrm{MVM}}(X)\mathrm{d}X \tag{15}$$

The mechanism by which carbon reacts with CO_2 is not yet fully understood. The reaction is widely accepted to proceed by the sorption of the reactant, the reaction on solid surface, and the desorption of the product. The simplest mechanism of the reaction is given by two steps, which are expressed by Eqs. 16–17:

$$C_f + CO_2 \underset{k_{-1}}{\overset{k_1}{\leftrightarrow}} C(O) + CO \tag{16}$$

$$C(O) \overset{k_2}{\rightarrow} CO + C_f \tag{17}$$

where C_f represents an active site and $C(O)$ an occupied site. Reaction (16) proceeds via CO_2 adsorption. When
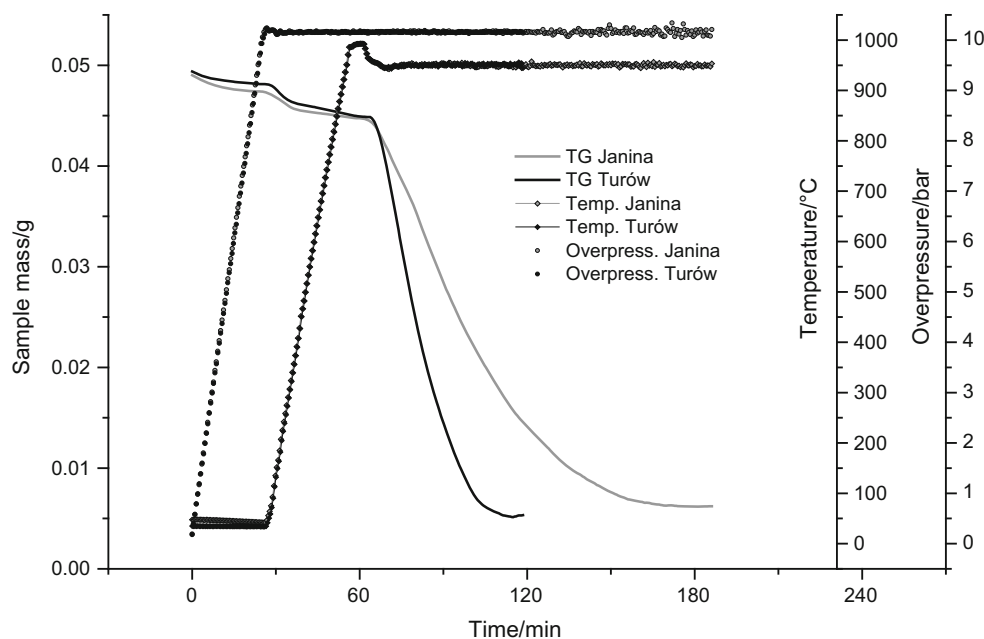
significant amounts of CO are present during the reaction, carbon monoxide acts as an inhibitor by reducing the steady-state concentration of the C(O) complexes in an inverse reaction. Reaction (17) describes the CO desorption where CO is removed from the occupied site on the carbon surface. The desorption step (Eq. 16) is considered much slower than the sorption step, thus it limits the global reaction rate. Ergun [21] proposed a rate equation for carbon-CO_2 gasification by using a *Langmuir–Hinshelwood rate expression*, given by Eq. 18, which involves the adsorption and desorption steps together with the effect of reactant pressures.

$$r = \frac{k_1 P_{CO_2}}{1 + \frac{k_1}{k_{-1}} P_{CO} + \frac{k_1}{k_2} P_{CO_2}} \qquad (18)$$

where k_1, k_{-1}, and k_2 are the kinetic constants, which depend on the temperature according to the Arrhenius law, and r represents the apparent reactivity. In the absence of CO, Eq. 18 simplifies to the following form:

$$r = \frac{k_1 P_{CO_2}}{1 + \frac{k_1}{k_2} P_{CO_2}} \qquad (19)$$

The reaction rate profiles are different for different carbonaceous material, i.e., they increase or decrease as the reaction proceeds and can also exhibit a maximum or minimum. Thus, the apparent reactivity should be chosen while considering this behavior. Normally, reactivity refers to a specific value of the conversion degree, such as 0.05 [22] or 0.5 [23]. However, using the representative value of the reactivity calculated by averaging the two conversion

degrees is also acceptable [14]. The most commonly used equation to calculate the reactivity is defined as follows and as can be seen it is connected with homogeneous model:

$$r = \frac{\frac{dX}{dt}}{1 - X}. \qquad (20)$$

Results and discussion

As mentioned before, the rate of coal char gasification toward CO_2 can by influenced by many process variables. The effect of temperature on carbon conversion for all studied temperatures and pressures is shown in Fig. 4a–h and for the Janina and Turów char, respectively. The carbon conversion curves show that the reaction rate increases linearly during the initial stages of conversion; the reaction slows and after the conversion reaches approximately 0.9 until the conversion is complete. The temperature significantly increases the gasification rate, and this trend is observed for both the Janina and Turów chars. Therefore, the time to complete the conversion is shortened by a factor of several dozens when comparing the processes at 850 and 1050 °C. The pressure also noticeably affects the gasification rate. A small increase in gasification reactivity was observed when increasing the pressure from 0.4 to 1 bar. Further increases in the CO_2 partial pressure resulted in significant increases of the reaction rate, especially at a pressure of 21 bar. The effect of the CO_2 partial pressure observed at 0.4 bar was likely obscured by the enhancing effect of the balance gas in the mixture (helium). As stated
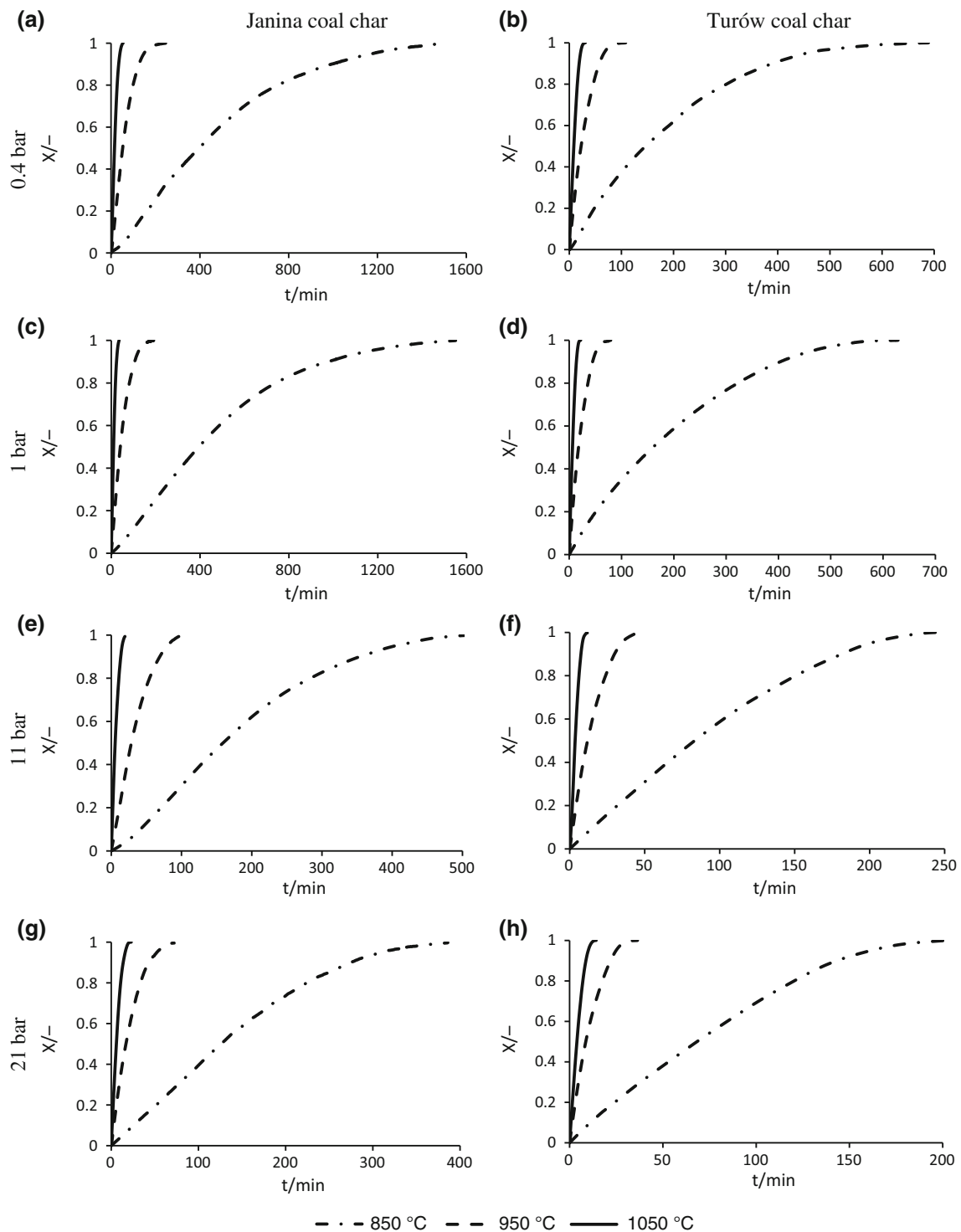
Fig. 4 Changes in the carbon conversion degree over time for different temperatures of the gasification of Janina (*left-hand side*) and Turów (*right-hand side*) coal chars, observed at CO_2 pressures of 0.4 (**a, b**), 1 (**c, d**), 11 (**e, f**), and 21 bar (**g, h**)

by Walker, Jr. et al. [24] and Zhang and Calo [25], the effect of the inert diluent gas on the measured kinetics cannot be neglected because the gas affects the active sites on the carbon matrix by changing their rate of rehybridization, thus changing the reactive lifetime of the active

site. The parent coal rank also noticeably affected the reactivity. When comparing the experimental data for same temperature and pressure conditions, char from less metamorphized parent coal (Turów) showed an approximately two times higher reactivity than a higher rank parent coal
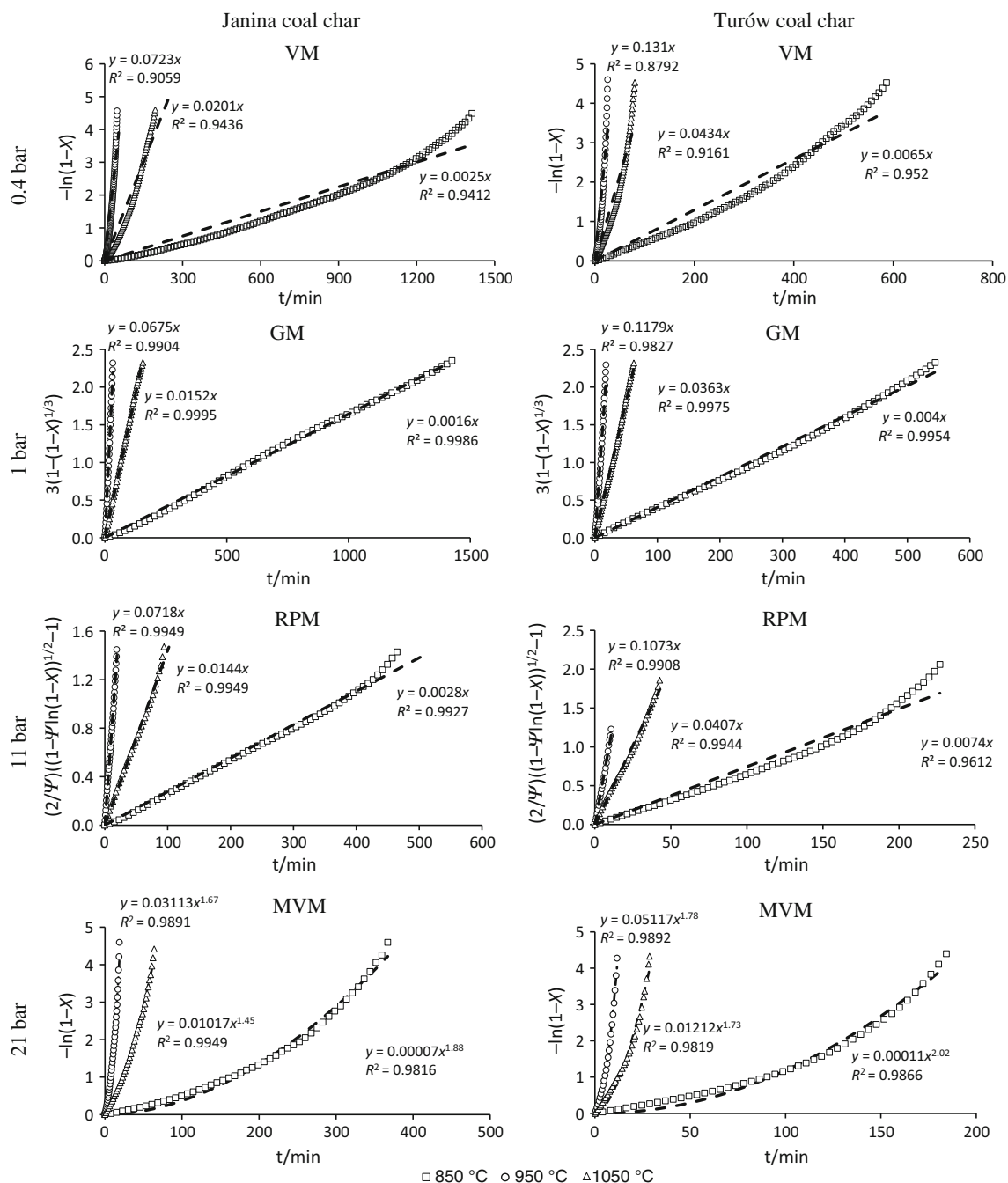
Fig. 5 Plots of the VM, GM, RPM, and MVM for the Janina (*left-hand side*) and Turów (*right-hand side*) coal char gasified at temperatures of 850, 950 and 1050 °C and CO_2 pressures of 0.4, 1, 11 and 21 bar

(Janina). Notably, the content of samples and the composition of mineral matter also differ among the coal samples.

To determine the best model to analyze the Arrhenius equation parameters, all aforementioned models were employed to describe the experimental data from this study. The VM, GM, RPM and MVM were compared together in one figure due to their simplicity for one pressure value. The results of the data prediction are

illustrated in Fig. 5. The experimental data used for the kinetic analyses covered conversion degrees ranging from 0 to 0.99. The determination coefficient R^2 was used to compare models and indicate the quality of the model fit. The VM yielded the poorest fit with the experimental data because the model failed to correctly predict higher conversion values, where the reaction rate is notably slower. The GM yielded a significantly improved fit, which

indicates that reaction mechanism is connected with the structural effects that occur while reaction proceeds. Equation 10 was used to calculate the structural parameter, ψ, in the RPM. This equation yielded ψ values between 2.0 and 2.6 for most of the Turów coal chars, which indicates that the reaction rate was maximized at similar conversion values. Furthermore, it directly indicates that the pore surface changes due to pore creation and coalescence of neighboring pores is maximized at similar conversion degrees. The same range of ψ values was determined for Janina coal char gasified at CO$_2$ pressures of 21 bar. The values of the structural parameter were notably higher (up to 6.3) for other temperature and pressure conditions employed to gasify Janina coal char, but in most cases, this parameter yielded values between 2 and 5. The structural

parameter ψ did not noticeably depend on the reaction temperature or pressure in either sample. The accurate fit of the MVM can also be explained in terms of the change in the pore surface. Compared to other models the MVM better predicts high conversion degrees, at which the rate is relatively small due to the collapse of the pore surface. The RPM together with the MVM yield similarly satisfactory fits, which agrees with previous studies where different thermobalance system was employed to study the CO$_2$ gasification kinetics [15]. Both the RPM and MVM are based on empirical outcomes but are still simple to apply to experimental data. Because the VM, GM and RPM equations are linear, the slope of the obtained lines equals the kinetic coefficients. The parameters a and b of the MVM were calculated by means of a non-linear curve fit with the

Table 3 Summary of values of empirical parameters, kinetic constants and determination coefficients for the VM, GM, RPM and MVM fitting to the experimental data of Turów coal char gasification under various temperature and pressure conditions

Press./bar	Temp./°C	VM		GM		RPM			MVM			
		k_{VM}/min^{-1}	R^2/–	k_{GM}/min^{-1}	R^2/–	Ψ/–	k_{RPM}/min^{-1}	R^2/–	a/–	b/–	k_{MVM}/min^{-1}	R^2/–
0.4	850	0.00646	0.9520	0.00409	0.9997	2.55	0.00333	0.9996	0.00046	1.44	0.00597	0.9961
	950	0.04349	0.9161	0.02815	0.9993	2.16	0.02406	0.9973	0.00334	1.63	0.04237	0.9893
	1050	0.13100	0.8792	0.08494	0.9944	2.28	0.07152	0.9923	0.00965	1.88	0.13743	0.9918
1	850	0.00615	0.9665	0.00404	0.9954	2.25	0.00340	0.9966	0.00011	1.66	0.00615	0.9852
	950	0.06659	0.9491	0.03719	0.9975	2.42	0.03058	0.9927	0.00505	1.63	0.05461	0.9908
	1050	0.17771	0.9530	0.11790	0.9827	2.47	0.09653	0.9934	0.01945	1.85	0.18834	0.9886
11	850	0.01321	0.9381	0.00888	0.9904	2.28	0.00745	0.9827	0.00007	2.02	0.01518	0.9807
	950	0.08503	0.9700	0.05428	0.9994	3.30	0.04054	0.9949	0.00955	1.63	0.08207	0.9919
	1050	0.34147	0.9438	0.21574	0.9912	10.38	0.10615	0.9949	0.04381	2.00	0.36361	0.9964
21	850	0.01679	0.9393	0.01112	0.9905	2.02	0.00968	0.9869	0.00011	2.02	0.01890	0.9892
	950	0.11436	0.9610	0.07490	0.9610	2.16	0.06399	0.9952	0.01212	1.73	0.11574	0.9849
	1050	0.28161	0.9589	0.18448	0.9963	2.37	0.15315	0.9950	0.05117	1.78	0.28661	0.9916

Table 4 Summary of values of empirical parameters, kinetic constants and determination coefficients for the VM, GM, RPM and MVM fitting to the experimental data of Janina coal char gasification under various temperature and pressure conditions

| Press./bar	Temp./°C	VM		GM		RPM			MVM			
		k_{VM}/min^{-1}	R^2/–	k_{GM}/min^{-1}	R^2/–	Ψ/–	k_{RPM}/min^{-1}	R^2/–	a/–	b/–	k_{MVM}/min^{-1}	R^2/–
0.4	850	0.00251	0.9412	0.00163	0.9997	5.19	0.00103	0.9991	0.00008	1.50	0.00238	0.9933
	950	0.02009	0.9436	0.01253	0.9993	2.93	0.00978	0.9999	0.00169	1.50	0.01852	0.9988
	1050	0.07158	0.9059	0.04668	0.9969	3.08	0.03565	0.9975	0.00580	1.70	0.07191	0.9956
1	850	0.00255	0.9801	0.00164	0.9904	3.07	0.00125	0.9996	0.00009	1.48	0.00241	0.9953
	950	0.02409	0.9797	0.01520	0.9995	2.71	0.01215	0.9996	0.00225	1.50	0.02244	0.9962
	1050	0.10294	0.9630	0.06744	0.9986	2.09	0.05807	0.9955	0.01025	1.72	0.10408	0.9934
11	850	0.00687	0.9560	0.00455	0.9952	5.99	0.00276	0.9927	0.00007	1.79	0.00723	0.9891
	950	0.03560	0.9678	0.02345	0.9986	5.82	0.01435	0.9949	0.00212	1.66	0.03576	0.9894
	1050	0.18429	0.9661	0.12022	0.9985	6.26	0.07177	0.9949	0.03062	1.72	0.18203	0.9912
21	850	0.00893	0.9510	0.00586	0.9940	2.37	0.00486	0.9925	0.00007	1.88	0.00950	0.9916
	950	0.05723	0.9828	0.03654	0.9998	2.14	0.03136	0.9996	0.01017	1.45	0.05322	0.9949
	1050	0.18242	0.9664	0.11828	0.9987	2.22	0.10021	0.9970	0.03113	1.67	0.17964	0.9891

least squares method (Eq. 13). The average value of the kinetic constant was then calculated by employing Eq. 15. The obtained parameters and kinetic constants are summarized in Tables 3 and 4 for the Janina and Turów coal char, respectively. Both tables show the data obtained at 0.4, 1, 11, and 21 bar and 850, 950, and 1050 °C.

The Langmuir–Hinshelwood expression is often used to predict the gasification rate observed at various pressures. It presents a significant advantage because it is applicable over a wider range of conditions than other models, e.g., the VM, GM, and RPM. However, the Langmuir–Hinshelwood kinetic model yields uncertain results at pressures above 1 bar. In these cases, extra steps are added to the reaction mechanism given by Eqs. 16 and 17. First, the representative reactivity was calculated according to Eq. 20 to confirm the validity of the LH equation to predict the kinetic behavior of the studied samples, and the average conversion degree ranging from 0.2 to 0.8 was chosen. The

relationships between these representative reactivities and the CO_2 pressure are illustrated in Fig. 6 for temperatures of 850, 950 and 1050 °C for both studied samples. To

Table 5 Kinetic coefficients calculated for Langmuir–Hinshelwood kinetics for Janina and Turów coal chars gasified at temperatures of 950, 950 and 1050 °C

Sample	Temp./°C	k_1/bar^{-1} min^{-1}	k_2/bar^{-1}	R^2/–
Janina coal char	850	0.0043	0.0084	0.9669
	950	0.0493	0.0443	0.8869
	1050	0.2460	0.1703	0.9954
Turów coal char	850	0.0117	0.0142	0.9425
	950	0.1196	0.0884	0.9468
	1050	0.3888	0.3152	0.9903
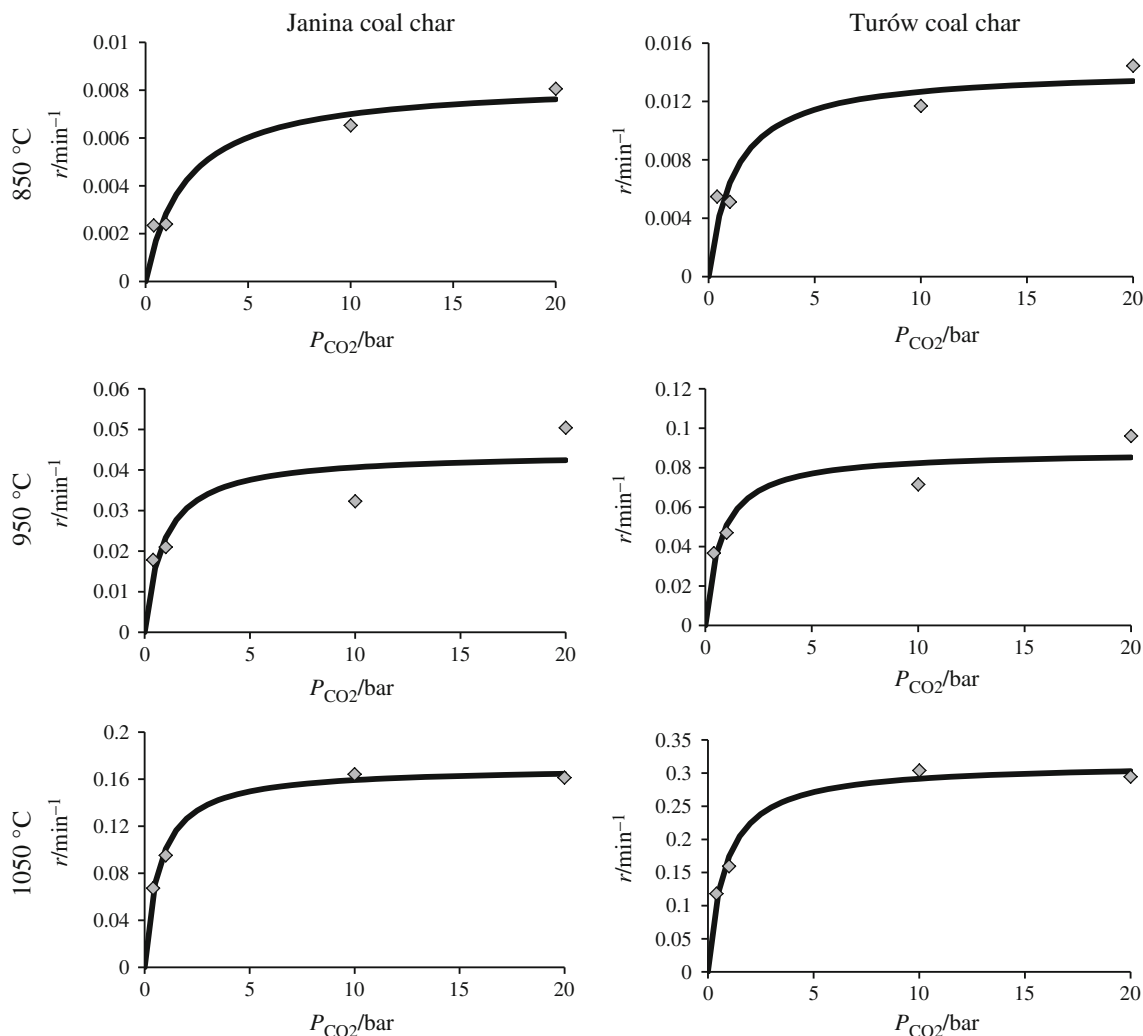
Fig. 6 Fitting of the LH expression for relationships between the representative reactivity and CO_2 pressures for the gasification of Janina (*left-hand side*) and Turów (*right-hand side*) coal chars at temperatures of 850, 950 and 1050 °C

Fig. 7 Relationship between conversion degree predicted by the VM, GM, RPM, MVM, and LH models for Janina (*left-hand side*) and Turów (*right-hand side*) coal chars at some exemplary temperature and pressure conditions
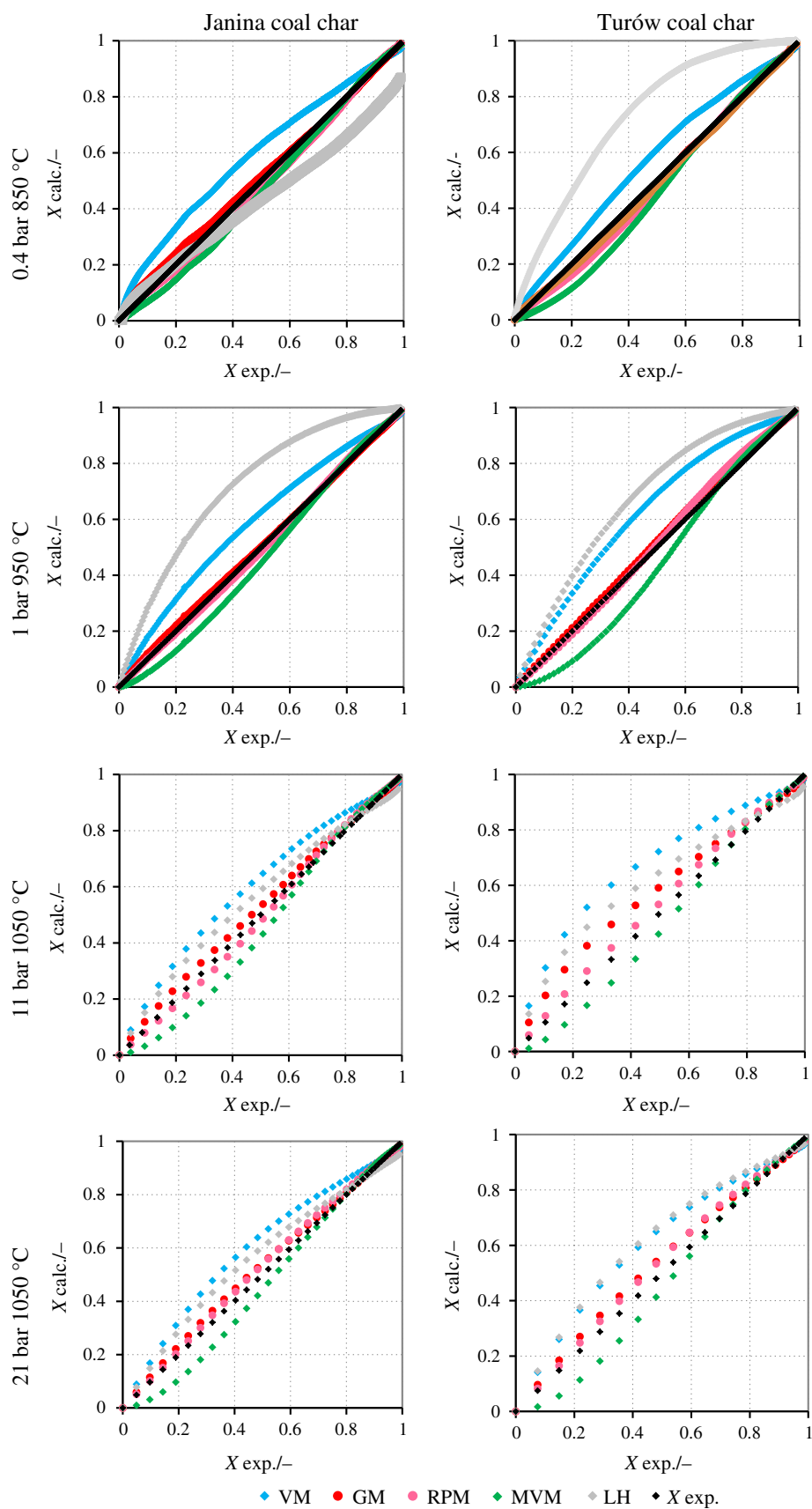
Table 6 Summary of kinetic expressions corresponding to VM, GM, RPM, MVM, and LH used for models' validation

Notation	Expression	Eq. number
VM (volumetric model)	$X = 1 - \exp(-k_{VM}t)$	(31)
GM (grain model)	$X = 1 - \left(1 - \frac{1}{3}k_{GM}t\right)^3$	(32)
RPM (random pore model)	$X = 1 - \exp\left(\frac{1}{\psi}\left(1 - \left(\frac{k_{RPM}t\psi}{2} + 1\right)^2\right)\right)$	(33)
MVM (modified volumetric model)	$X = 1 - \exp(at^b)$	(34)
L–H model (Langmuir–Hinshelwood model)	$X = 1 - \exp\left(-\frac{k_1 P_{CO_2}t}{1 + \frac{k_1}{k_{-1}}P_{CO} + \frac{k_1}{k_2}P_{CO_2}}\right)$	(35)

Table 7 Values of absolute deviation of the z intercept for VM, GM, RPM, MVM, and LH models describing the gasification behavior of Janina coal char

Pressure/bar	Temp./°C	VM	GM	RPM	MVM	LH
0.4	850	1.049	1.002	0.991	0.991	0.849
	950	1.054	1.003	1.004	0.995	1.090
	1050	1.066	1.019	1.018	0.991	1.218
1	850	1.049	1.002	1.000	0.992	1.212
	950	1.051	1.000	1.001	0.991	1.157
	1050	1.068	1.020	1.025	0.988	1.176
11	850	1.071	1.023	1.012	0.986	1.078
	950	1.060	1.013	1.001	0.985	1.098
	1050	1.064	1.016	1.004	0.984	1.017
21	850	1.067	1.024	1.027	0.985	0.988
	950	1.045	0.997	1.001	0.991	0.936
	1050	1.062	1.013	1.017	0.985	1.019
$\sum|1 - z|_{T,p}$		0.706	0.132	0.101	0.136	0.838

estimate the model parameters, the reaction was assumed to be prevented by $P_{CO_2} = 0$.

Figure 6 shows that an apparent shift in the reaction order can be distinguished as the CO_2 pressure is increased. The LH model appears applicable, particularly for the relationships observed at 1050 °C for the Janina and Turów coal chars. The shifts of the reaction order are still present at lower temperatures, but the significant inconsistencies are observed at 11 and 21 bar. The LH model expression explains the saturation effect of the reaction surface, which desensitizes the rate to pressure increases. This desensitization occurs because the surface is maximally

Fig. 8 Arrhenius plots for the kinetic constants corresponding to the ▶ VM, GM, RPM, MVM for Turów (*left-hand side*) and Janina (*right-hand side*) coal chars gasified at CO_2 pressures of 0.4 (**a, b**), 1 (**c, d**), 11 (**e, f**), and 21 bar (**g, h**)

concentrated with C(O) complexes, and further increases in the CO_2 pressure do not impact their concentration or the reaction rate. Saturation was observed for both samples gasified at 1050 °C. Nevertheless, the reactivity notably increased when the pressure was increased from 11 to 21 bar at 850 and 950 °C. This effect is not fully understood because the apparent reaction order for these pressure ranges was observed to be nearly zero [26]. The values of kinetic constants k_1 and k_2 were calculated directly by non-linear estimation using the Levenberg–Marquardt method. The resultant values corresponding to both samples and temperatures of 850, 950, and 1050 °C are given in Table 5.

Models' validation

Analyzing the data given in Tables 3 and 4, it could be concluded that all *n*th-order models, excepting the VM, represent very well the reactivity behavior in the wide range of conversion degree ranging from 0 to 0.99 for both samples at all pressure and temperature conditions. In case of Langmuir–Hinshelwood kinetics, due to a fact that reactivity representative value being mean for conversion degree from 0.2 to 0.8 was taken instead of reaction rate it can be thought that this model will not predict the

Table 8 Values of absolute deviation of the z intercept for VM, GM, RPM, MVM, and LH models describing the gasification behavior of Turów coal char

Pressure/bar	Temp./°C	VM	GM	RPM	MVM	LH
0.4	850	1.045	0.995	0.996	0.990	1.171
	950	1.060	1.009	1.013	0.983	1.197
	1050	1.079	1.028	1.033	0.983	1.237
1	850	1.059	1.010	1.013	0.979	1.215
	950	1.105	1.019	1.019	0.983	1.152
	1050	1.075	1.026	1.028	0.982	1.202
11	850	1.083	1.033	1.037	0.974	1.068
	950	1.060	1.009	1.006	0.984	1.050
	1050	1.091	1.033	1.021	0.986	1.031
21	850	1.085	1.034	1.040	0.976	0.980
	950	1.064	1.013	1.018	0.977	0.947
	1050	1.072	1.023	1.026	0.985	1.082
$\sum|1 - z|_{T,p}$		0.878	0.232	0.250	0.218	1.332

Turów coal char

Janina coal char
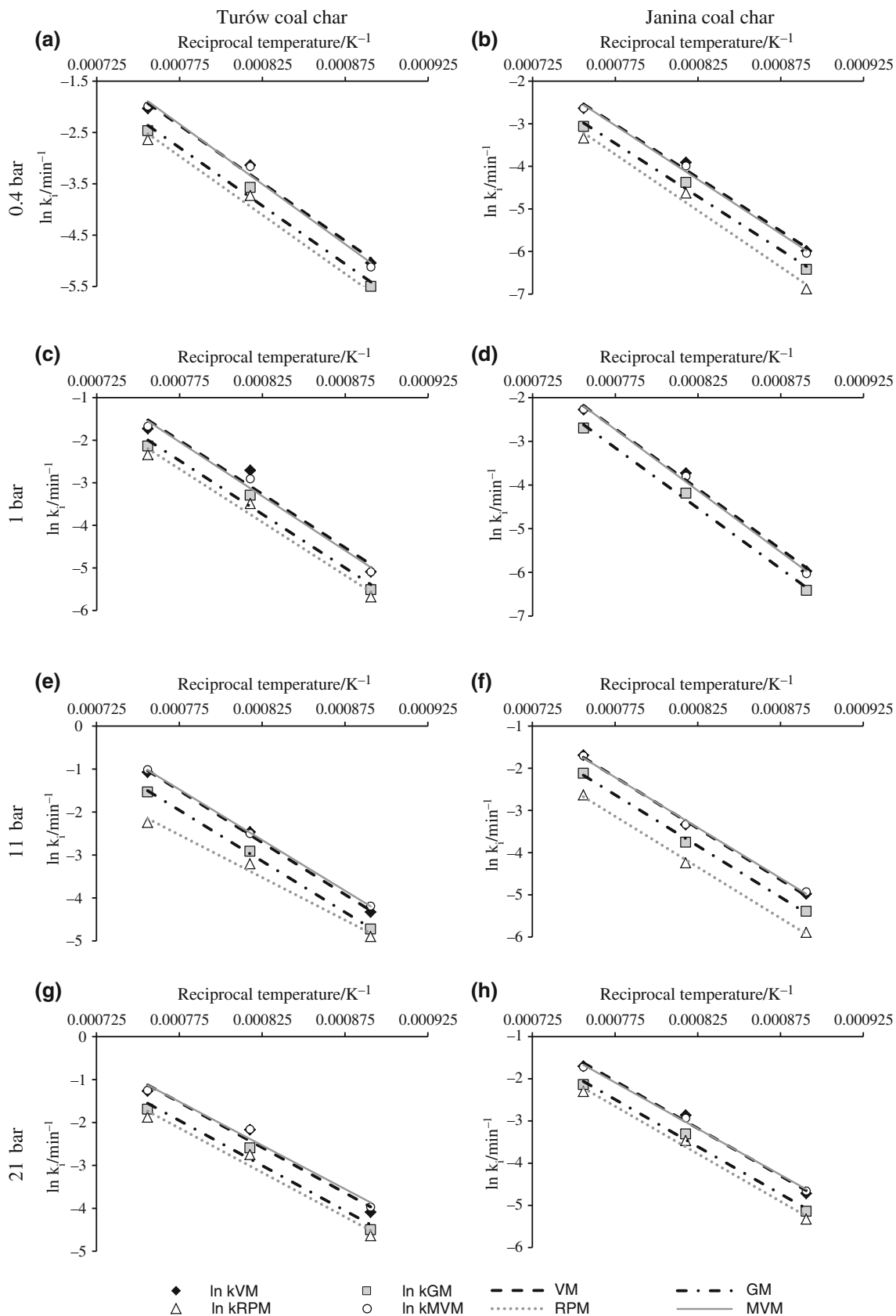
Fig. 9 Arrhenius plots for the kinetic constants determined by employing Langmuir–Hinshelwood expression
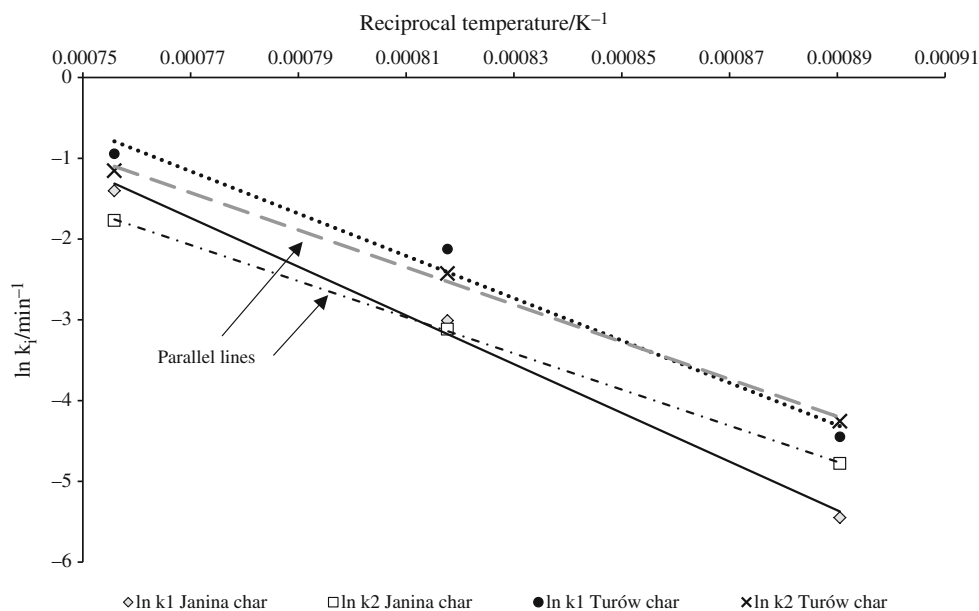
conversion versus time relationship very well. In order to compare the models in a reliable manner, we collated the data representing relationships of calculated conversion degree versus experimental conversion degree, what was shown in Fig. 7 for some randomly selected temperature and pressure conditions. For the calculation of conversion degree, formulas presented in Table 6 were used. In order to express the goodness of prediction of conversion degree, we decided to employ linear relationship of X calc. $= z \cdot X$ exp., where z is the slope calculated by means of linear regression with least squares method. Since for ideal case the X calc. $= X$ exp., then the closer the value of z to 1, the better particular model predicts the experimental data.

In Tables 7 and 8, we gathered the absolute values of z coefficients for all temperature and pressure conditions for Janina and Turów coal char, respectively. Some sample-type influences can be noticed because the sum of deviations is always higher for Turów than for Janina coal char. It can be seen that two models—VM and LH, are considered as giving the poorest fitting for both samples due to the highest values of the absolute deviations of the z slope. Interestingly, the lowest value of the sum observed for each sample varies with model, which could be interpreted as connected with different mechanisms of reaction. For the Janina coal char, the best result was obtained with random pore model, while for Turów coal char the best-fitting is the modified volumetric model. It can be concluded that for the higher rank Janina coal char, the mechanism can be connected with very poor initial surface area evolving and collapsing with extend of reaction, and thus the best outcomes are observed the RPM. However,

for the Turów char derived from low-rank lignite having already sufficiently developed pore surface area and high content of mineral species responsible for catalytic and inhibiting effects, the mechanism of reaction could be so complicated that it can be described well only by empirical kinetic equation.

The Arrhenius equation parameters (activation energy and pre-exponential factor) were calculated for all analyzed models. The VM-, GM-, RPM-, MVM- and L–H-based kinetic constants can be related to the absolute temperature according to the relationship given by Eq. 3. Figure 8 shows the Arrhenius plots for all of the kinetic coefficients for the VM, GM, RPM, MVM. The Arrhenius relationship for the LH-derived kinetic constants are gathered together for both analyzed samples and illustrated in Fig. 9. The relationships for the nth-order models are divided to the left- and right-hand side for the Turów and Janina coal char, respectively. The vast majority of Arrhenius plots create parallel lines, indicating similar values of the activation energy obtained from different kinetic expressions. The GM and the RPM yield lines parallel to the MVM. However, the RPM shows a significant discrepancy for the Turów char gasified at 11 bar (Fig. 8e). The Arrhenius relationships obtained for the LH-type kinetic expression distinctly shows the effect of parent coal rank on the value of the activation energy of the k_1 constant. However, the relationships obtained for k_2 for the Janina and Turów coal char yield parallel lines. This relationship indicates that the rate of the desorption step in the LH mechanism (represented by the kinetic constant k_2) is not connected with the coal rank but more likely with the applied process conditions. In summary, the calculated values of the activation

Table 9 Summary of the Arrhenius law parameters obtained for various kinetic expressions for the Turów and Janina coal chars at pressures of 0.4, 1, 11 and 21 bar

Model	VM		GM		RPM		MVM		L–H			
									k_1		k_2	
Press./ bar	$E/$ kJ mol⁻¹	$A \times 10^{-9}/$ min⁻¹	$E/$ kJ mol⁻¹	$A \times 10^{-6}/$ min⁻¹	$E/$ kJ mol⁻¹	$A \times 10^{-6}/$ min⁻¹	$E/$ kJ mol⁻¹	$A \times 10^{-6}/$ min⁻¹	$E/$ kJ mol⁻¹	$A \times 10^{-8}/$ min⁻¹	$E/$ kJ mol⁻¹	$A \times 10^{-6}/$ min⁻¹
Turów coal char												
0.4	186.81	3.44	188.25	2.55	190.51	2.67	194.58	7.28	217.82	1.81	191.97	12.65
1	209.64	41.20	209.73	25.96	207.93	17.98	212.48	52.06				
11	201.21	31.19	197.33	13.75	164.97	0.38	196.08	19.85				
21	175.47	2.75	174.76	1.69	171.84	1.08	169.06	1.53				
Janina coal char												
0.4	207.83	12.67	208.13	8.36	219.7T4	19.06	211.17	16.86	250.77	21.45	185.98	3.80
1	229.22	126.31	230.20	89.46	237.53	148.94	233.34	182.44				
11	202.71	17.70	201.73	10.58	200.77	5.82	198.79	12.20				
21	187.09	4.82	186.27	2.88	187.61	2.78	182.00	2.89				

energy and pre-exponential factor for both samples and all models and pressures are gathered in Table 9.

For all studied kinetic expressions and applied pressure conditions, the values of the activation energy ranged from 165 to 212 kJ mol⁻¹ for the Turów coal char and 186 to 238 kJ mol⁻¹ for the Janina coal char. This agrees with the data reported in the literature. However, the activation energies for Janina coal char seem to be too small taking into account way higher rank of this fuel as compared to Turów lignite. The slightly higher values for the Janina coal char do not represent the real diversity in the reactivity between studied samples. However, this diversity is given by the values of pre-exponential factor, which takes into account the pore surface and mineral matter effects which are considerably different for both samples. The activation energies calculated for the same pressure conditions but with different models are similar, and the differences are less than 20 kJ mol⁻¹, indicating that the "real" activation energy likely falls in this range. For the L–H-type expression, the differences in the rank of the parent coal are manifested in the k_1 constant. Thus, the activation energies were 218 and 251 kJ mol⁻¹ for the Turów and the Janina coal char, respectively. As mentioned above, the activation energies corresponding to the kinetic coefficient k_2 are similar and vary from 186 to 192 kJ mol⁻¹.

Conclusions

The CO₂ gasification rates of two coal chars derived from Polish sub-bituminous coal and lignite were studied experimentally. Twenty-four tests were performed in a pressurized thermogravimetric analyzer between 850 and 1,050 °C and pressures of 0.4, 1, 11, and 21 bar. The char derived from the lower rank lignite was approximately two times more reactive (in terms of the time needed to complete reaction) than the sample derived from sub-bituminous coal. Increases in temperature and pressure significantly affected the rate of gasification observed for both samples. However, increases in the temperature affected the reaction rate much more dramatically than increases in pressure.

To perform a comprehensive kinetic analysis, five models were used to describe the kinetic behavior of studied the samples: the VM, GM, RPM, MVM, and Langmuir–Hinshelwood models were used. The most general Langmuir–Hinshelwood model was applicable to all pressures, even though it is not recommended for pressures higher than 1 bar. The results were found to be satisfactory, especially at 1050 °C, when both samples showed a saturation effect at 11 and 21 bar.

The validity of these models was examined after analyzing their fit with the experimental data, by plotting

predicted value of conversion degree, X calc., against experimental extent of reaction, X exp., and calculating values of slope for each relationship by using least squares method. The sum of absolute deviations of the z value from ideal case, when $z = 1$, was found to be adequate indicator of model applicability. The results obtained for the VM and LH were considered unsatisfactory, but the results from the GM, RPM and MVM were significantly better, especially for the last two models. It was established that for the Janina coal char the reactivity behavior was very well predicted by means of RPM, and for the Turów coal char by the MVM. These differences were explained by means of significantly different rank, and therefore, the properties of the samples.

The calculated values of the activation energy were similar for the various models used, and ranged from 165 to 212 kJ mol^{-1} for the Turów char and 186 to 238 kJ mol^{-1} for the Janina coal char. For the Langmuir–Hinshelwood kinetics, the activation energy for the formation of active complexes was a function of the rank of the parent coal and was higher for more altered coal char (218 and 251 kJ mol^{-1} for Turów and Janina char, respectively). The activation energy of the second step was found to be lower than that of the first step, and the values were similar for both coal chars and ranged from 186 to 192 kJ mol^{-1}.

References

1. Zhou Z, You Z, Wang Z, Hu Z, Zhou J, Cen K. Process design and optimization of state-of-the-art carbon capture technologies. Environ Prog Sustain Energy. 2014;33:993–9.
2. Stec M, Spietz T, Więcław-Solny L, Tatarczuk A, Wilk A. Density of unloaded and CO_2-loaded aqueous solutions of piperazine and 2-amino-2-methyl-1-propanol and their mixtures from 293.15 to 333.15 K. Phys Chem Liq. 2016;54:475–86.
3. Tomaszewicz G, Kotyczka-Morańska M. Study on Ca-based sorbents for CO_2 capture from process gases. Przem Chem. 2013;92:1719–24.
4. Kotyczka-Moranska M, Tomaszewicz G. Application of polish calcium sorbents in carbonate looping. Physicochem Probl Miner Process. 2013;49:111–20.
5. Siriwardane RV, Ksepko E, Tian H, Poston J, Simonyi T, Sciazko M. Interaction of iron–copper mixed metal oxide oxygen carriers with simulated synthesis gas derived from steam gasification of coal. Appl Energy. 2013;107:111–23.
6. Ksepko E, Babinski P, Evdon A, Nalbandian L. Studies on the redox reaction kinetics of selected, naturally occurring oxygen carrier. J Therm Anal Calorim. 2016;124:137–50.
7. Ksepko E. Examining $SrCuO_2$ as an oxygen carrier for chemical looping combustion. J Therm Anal Calorim. 2015;122:621–33.
8. Babiński P, Łabojko G, Kotyczka-Morańska M, Plis A. Kinetics of coal and char oxycombustion studied by TG–FTIR. J Therm Anal Calorim. 2013;113:371–8.
9. Lasek J, Janusz M, Zuwala J, Glod K, Iluk A. Oxy-fuel combustion of selected solid fuels under atmospheric and elevated pressures. Energy. 2013;62:105–12.
10. Chmielniak T, Sciazko M, Tomaszewicz G, Tomaszewicz M. Pressurized CO_2-gasification of coal. J Therm Anal Calorim. 2014;117:1479–88.
11. Molina A, Mendragon F. Reactivity of coal gasification with steam and CO_2. Fuel. 1998;77:1831–9.
12. Irfan MF, Usman MR, Kusukabe K. Coal gasification in CO_2 atmosphere and its kinetics since 1948: a brief review. Energy. 2011;36:12–40.
13. Roberts DG, Harris DJ. A kinetic analysis of coal char gasification reactions at high pressures. Energy Fuels. 2006;20:2314–20.
14. Fermoso J, Stevanov C, Moghtaderi B, Arias B, Pevida C, Plaza MG, Rubiera F, Pis JJ. High-pressure gasification reactivity of biomass chars produced at different temperatures. J Anal Appl Pyrolysis. 2009;85:287–93.
15. Tomaszewicz M, Łabojko G, Tomaszewicz G, Kotyczka-Morańska M. The kinetics of CO_2 gasification of coal chars. J Therm Anal Calorim. 2013;113:1327–35.
16. Soreanu G, Tomaszewicz M, Fernandez-Lopez M, Valverde JL, Zuwała J, Sanchez-Silva L. CO2 gasification process performance for energetic valorization of microalgae. Energy. 2017;119:37–43. doi:10.1016/j.energy.2016.12.046.
17. Ishida M, Wen CY. Comparison of zone-reaction model and unreacted-core shrinking model in solid–gas reactions—I isothermal analysis. Chem Eng Sci. 1971;26:1031–41.
18. Szekely J, Evans JW. A structural model for gas-solid reactions with moving boundary. Chem Eng Sci. 1970;25:1091–107.
19. Bhatia SK, Perlmutter DD. A random pore model for fluid-solid reactions: I. Isothermal, kinetic control. AIChE J. 1986;72:797–803.
20. Kasaoka S, Sakata Y, Tong C. Kinetic evaluation of the reactivity of various coal chars for gasification with carbon dioxide in comparison with steam. Int Chem Eng. 1985;25:160–75.
21. Ergun S. Kinetics of the reaction of carbon dioxide with carbon. J Phys Chem. 1956;60:480–5.
22. Chen G, Yu Q, Sjostrom K. Reactivity of char from pyrolysis of birch wood. J Anal Appl Pyrolysis. 1997;40–41:491–9.
23. Ollero P, Serrera A, Arjona R, Alcantarilla S. The CO_2 gasification kinetics of olive residue. Biomass Bioenergy. 2003;24:151–61.
24. Walker PL Jr, Pentz L, Biederman DL, Vastola FL. The influence of "inert" diluent gases on the rate of carbon gasification. Carbon. 1977;15:165–8.
25. Zhang L, Calo JM. The "inert gas effect" on carbon reactivity. In: Proceedings of the 1995-22nd Biennial Carbon Conference. San Diego: University of California; 1995. p. 602–6.
26. Roberts DG, Harris DJ. Char gasification with O2, CO2, and H2O: effects of pressure on intrinsic reaction kinetics. Energy Fuels. 2000;14:483–9.